Long-term trends and solar response of the mesopause temperatures observed by TIMED/SABER during the 2002-2019 period

X. R. Zhao[1], Z. Sheng[1,2*], H. Q. Shi[1], L. B. Weng[1], and Q. X. Liao[1]

[1] College of Meteorology and Oceanography, National University of Defense Technology, Nanjing, China.

[2] Collaborative Innovation Center on Forecast and Evaluation of Meteorological Disasters, Nanjing University of Information Science and Technology, Nanjing, China.

Corresponding author: Zheng Sheng (19994035@sina.com)

Key Points:

- The mesopause temperature during 2002-2019 shows a cooling trend through all latitudes ranging from -0.002 to -0.113 K/year.
- The mesopause temperature shows a positive response to solar activity through all latitudes ranging from 2.74 to 4.76 K/100sfu.
- A long enough length of the time interval for analysis is the main factor guarantying the quality of the results.

Abstract

The global distribution and variations of the monthly mesopause temperature are presented during 2002-2019 covering the latitudes of 83°S-83°N based on Sounding of the Atmosphere using Broadband Emission Radiometry (SABER) observations. To investigate the long-term trend and solar response of the mesopause temperature, a three-component harmonic fit is first applied to remove the seasonal variation from the monthly temperature data series. Then a multiple linear regression model is performed to residual temperatures versus constant, time series, solar activity, and geomagnetic activity terms. In this study, the mesopause temperature shows a cooling trend through all latitudes ranging from -0.002 to -0.113 K/year with a mean of -0.069 ± 0.036 K/year. The cooling trends in the southern hemisphere are observed to be relatively stronger than those in the northern hemisphere. For high latitudes (60°–80°), significant negative trends can be detected during the non-summer time, while no significant trends are found for summertime. The mesopause temperature shows apparent positive responses to solar activity through all latitudes ranging from 2.74 to 4.76 K/100sfu with a mean of 3.94 ± 0.59 K/100sfu, which are more significant and stable in the northern hemisphere. There is a pronounced drop in solar response near the equator, which could be caused by tidal forcing at low latitudes. It is noteworthy that the length of the time interval for analysis is the main factor influencing the quality of the results. Our results, using an eighteen years interval, are expected to be a robust reference for the mesopause temperature variations.

1. Introduction

The mesopause is the transition between the mesosphere and the thermosphere, which is located at “the altitude of the absolute minimum in the temperature” (She & Zahn, 1998). The mesopause layer separates two distinct dynamical regions of the upper atmosphere: the mesosphere, where atmospheric processes are mainly dominated by internal variability caused by upward propagating waves; and the thermosphere, which is mainly influenced by external solar effects. The thermal structure of the mesopause controlled by a complex interaction of dynamics, radiative transfer, and photochemistry (Smith, 2004). In general, the energy budget in the vicinity of the mesopause is governed primarily by radiative processes. Adiabatic heating and cooling mechanisms by the general circulation, transport of heat by convective instability and energy deposition by gravity waves also play important roles in the energetics of the mesopause region (Brasseur & Solomon, 2005). Previous studies have suggested that human-induced emissions of carbon dioxide and methane could also lead to mesopause perturbations. It has been revealed by Roble and Dickinson (1989) that the increase of greenhouse gases leads to cooling in the middle atmosphere. Beig et al. (2003) summarized that if greenhouse gas (CO_2) concentrations were doubled, the temperature in the mesopause region (80 – 100 km) would be decreased by 5 – 6 K on a globally averaged basis.

Determination of the mesopause temperature long-term trend and solar response is a necessary but rather challenging task, primarily because of the limited sampling and a limitation in length of data records. However, in recent decades, many observations have been conducted to estimate the long-term variation of the mesopause region (80 – 100 km) temperature and its response to solar activity. According to rocket research, long-term cooling at heights of 25 – 90 km was showed by Semenov et al. (2002) suggesting systematic subsidence of the upper atmospheric layers. Berger and Lübken (2011) reported a cooling trend on the order of 2 – 4 K/decade in the mesosphere during 1961 – 2009 by using the Leibniz-Institute Middle Atmosphere (LIMA) model and, for the first time, confirmed the extraordinarily large trends from observations with the modeling of mesospheric temperature trends. Based on the analysis of the LIMA model results, Lübken et al. (2013) revealed that CO_2 is the main driver of cooling trends in the mesosphere, whereas O_3 contributes approximately one third. She et al.(2015) deduced the long-term midlatitude temperature trend from 1990 to 2014 of Na lidar observations and exhibited a cooling trend of 0.64 ± 0.99 K/decade at 85 km, increasing to a maximum of 2.8 ± 0.58 K/decade between 91 and 93 km, and then shifting to a warming trend above 103 km. As for the solar response, Forbes et al. (2014) conducted an analysis of the middle atmosphere temperatures, measured by SABER during 2002 – 2013, on both fixed altitude and fixed pressure levels and reported a detectable solar dependence of 3 – 5 K/100 solar flux units (sfu) at 80 – 90 km occurring between $\pm 60°$ latitude. The satellite analysis of Tang et al. (2016) indicates that the global solar response of the mesopause temperature is 4.89 ± 0.67 K/100sfu based on the Sounding of the Atmosphere using Broadband Emission Radiometry (SABER) observations for the period of 2002 – 2015. Some researchers reported both two works at the same time. Offermann et al (2010) analyzed annual mean hydroxyl (OH) temperatures at Wuppertal (51°N, 7°E) and found a long-term trend of -0.23 K/year and a solar flux sensitivity of 0.035 K/sfu for the time interval of 1988 – 2008. Kalicinsky et al. (2016) also reported a cooling trend of -0.089 ± 0.055 K/year and a significant positive sensitivity to the solar activity of 4.2 ± 0.9 K/100sfu in the mesopause region at Wuppertal (51°N, 7°E) by analyzing the OH temperature data series from 1988 to 2015. The Na lidar observations at 41°N during 1990 – 2018 of Yuan et al. (2019) indicated a cooling trend of 2.5 ± 0.4 K/decade for the “high mesopause” (HM) and a similar 2.3 ± 0.5 K/decade cooling trend for the “low mesopause” (LM), while that during 2000-2018 shows a statistically insignificant trend of -0.2 ± 0.7 K/decade and -1 ± 0.9 K/decade for the HM and the LM, respectively. And the lidar data also demonstrated a large response to solar flux variation of 0.03 ± 0.1 K/sfu for the LM and 0.01 ± 0.007 K/sfu for the HM. The reviews of temperature trend and its solar response in the mesosphere is summarized by Beig et al. (2003; 2006; 2008; 2011a; 2011b). It appears that the long-term temperature trends as well as its solar responses in the mesosphere are not uniform in magnitude but mostly agree in sign with the negative temperature trend and the positive solar response.

The reported long-term temperature trends and solar responses mostly focus on certain locations, and the researches covering a global scale with respect to the mesopause temperature variation are relatively rare. However, with a larger scope and longer records, SABER onboard the Thermosphere Ionosphere Mesosphere Energetics and Dynamics (TIMED) satellite provide a high-quality data source for the global mesopause temperature, thus producing an opportunity for quantitative assessment of mesopause temperature long-term trend and solar response. In this paper, using SABER data spanning from February 2002 to August 2019, we obtain the monthly mesopause temperatures from 83°N to 83°S with every 10° interval first, and then investigate their long-term trends and solar responses.

Section 2 provides an overview of the data sets used and describes the analysis methods in detail, including a harmonic fit with annual, semiannual and terannual components and a multiple linear regression model. Section 3 presents the results and discussion. Section 4 provides some further discussion, and Section 5 provides the concluding remarks.

2. Data and Method

2.1 Data Sets

The kinetic temperature data used in this paper were measured by the SABER instrument onboard the TIMED satellite, which was launched in December 2001. The TIMED orbits at an altitude of about 625km with an orbital inclination of 74.1° and makes 15 orbits per day with a period of 1.6 h. Thus, it takes about 60 days to complete full 24-hour coverage of local time (Russell et al., 1999). SABER has become one of the longest (18 years since 2002) operating infrared sensors, providing about 1400 vertical profiles of kinetic temperature a day from the tropopause to the lower thermosphere region. The latitude coverage of the SABER limb scan is 83°N-52°S or 52°N-83°S, with alternating coverage due to the spacecraft yaw cycle every 60 days. More detailed descriptions of the SABER instrument and the data retrievals can be found in Remsberg et al. (2008) and Mertens et al. (2009). The SABER data were downloaded from http://saber.gats-inc.com/.

In this paper, the TIMED/SABER version 2.0 temperature data were used for the period from February 2002 to August 2019 to obtain the mesopause temperatures. Every vertical profile of temperature was first linear interpolated at each 0.2 km in altitude from 40 km to 100 km and binned in a 10° latitudinal band from 83°S to 83°N. Then, the monthly averaged temperature profiles were calculated; actually, the monthly averages are the 60-day means centered on the fifteenth of each month. This averaging can mostly eliminate the influence caused by the migrating tides since SABER takes 60 days to cover all 24-hour local time at one given location. And then, the cold point mesopause (the altitude of the absolute minimum in the temperature, (She & Zahn, 1998)) and the corresponding mesopause temperature of each monthly averaged zonally temperature profiles were determined. For each latitude bin, repeating this process for each month during 2002-2019, a time series of the monthly means of mesopause temperature was formed in every 10° zonal band between 83°S - 83°N as shown in Figure 1. There are some missing measurements months at high latitudes (52°N-83°N or 52°S-83°S) due to the yaw cycle of SABER, which usually are April, August or December in the northern hemisphere; February, June or October

in the southern hemisphere. Additionally, the data series shows large gaps of several months due to technical problems in the years 2014 and 2015. These missing months have been excluded from the following analysis. Figure 1 clearly presents the presence of a pronounced annual variation with high temperatures during winter and low temperatures during summer at middle and high latitudes, which is consistent with other researchers reports (e.g., Lübken & von Zahn, 1991; She & von Zahn, 1998; Berger & von Zahn, 1999; Xu et al., 2007; Venkat Ratnam et al., 2010; Kalicinsky et al., 2016).

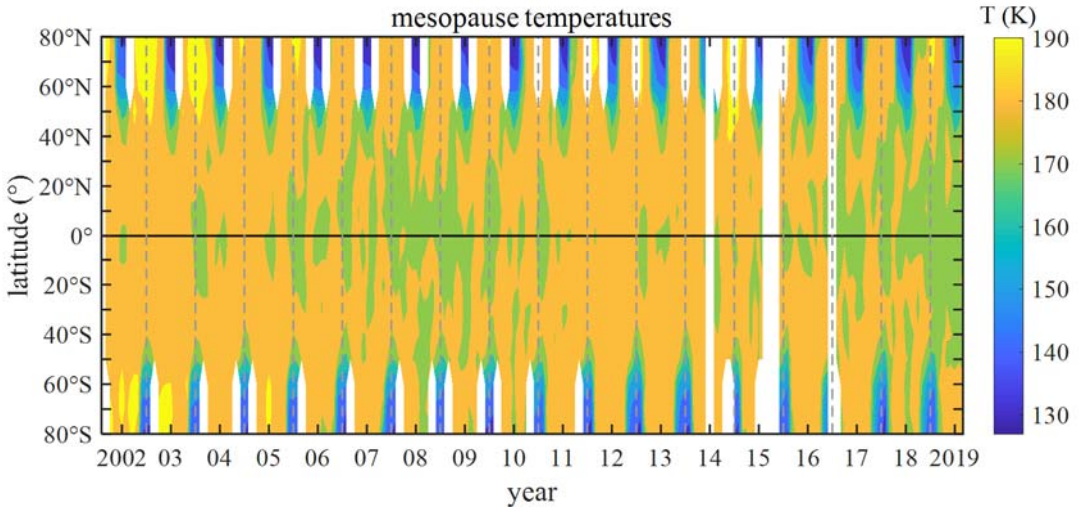

Figure 1. Monthly averaged mesopause temperatures derived from SABER measurements for different latitude bins as a function of the time of the month from February 2002 to August 2019. The blank gaps are due to data missing.

The solar radio flux index F10.7 (daily) and Kp index (three hourly) from 2002 to 2019 are used as proxies for solar extreme ultraviolet (EUV) radiation and geomagnetic activity, respectively. F10.7 flux index is commonly used as an indicator of solar activity in many middle and upper atmospheric temperature trend studies (Forbes et al., 2014; Yuan et al., 2019). The average F10.7 is calculated as

$$\mathrm{F10.7} = (\mathrm{F10.7_{adj}} + \mathrm{F10.7_{ctr81}})/2 \quad (1)$$

where $\mathrm{F10.7_{adj}}$ is 10.7 cm solar radio flux which has been adjusted to 1 AU and expressed in units of $10^{-22}\,\mathrm{W/m^2/Hz}$. $\mathrm{F10.7_{ctr81}}$ is an 81-day arithmetic average of daily adjusted F10.7 index, centered on the day of interest. This average F10.7 can be suitable for describing solar activity variation (Richards et al., 1994). F10.7 and Kp were downloaded from http://celestrak.com/SpaceData/. Monthly means of the F10.7 index and Kp index are computed for each month, yielding 212 points. Taking temperature data in the 70°N, 40°N, and 10°N latitude bins from Figure 1 to represent the high-, mid- and low- latitude areas, respectively, we plot their monthly time series in Figure 2 together with the associated F10.7 and Kp indices. Similar to the height of the mesopause, mesopause temperatures at high latitudes also present low summer level as shown in Figure 2(a). The blue points in Figure 2 are yearly averages. The solar cycle in yearly mesopause temperature can be easily seen.

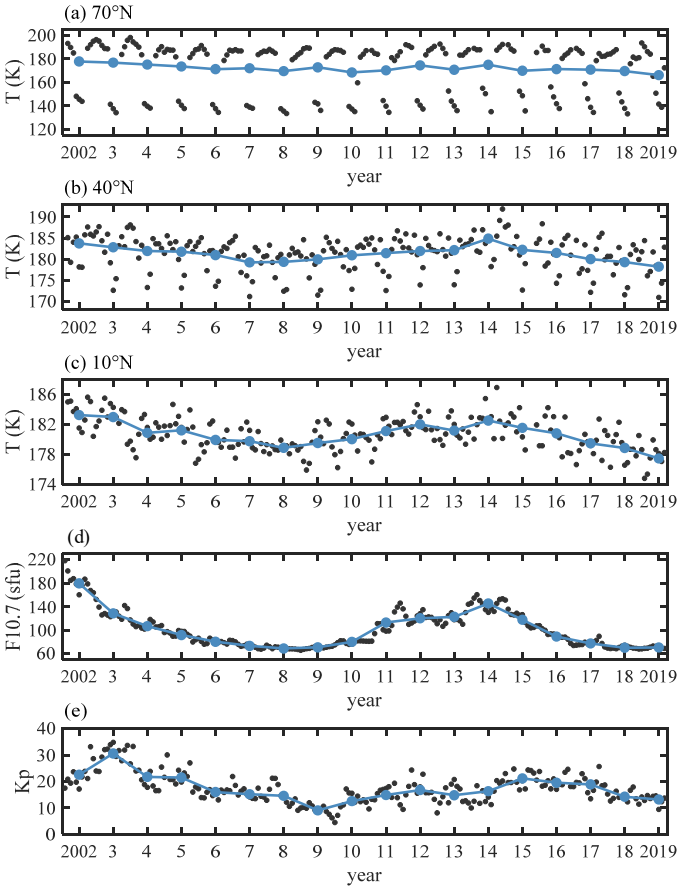

Figure 2. Long-term observational monthly mesopause temperatures derived from SABER in different latitude bins (a) 70°N, (b) 40°N and (c) 10°N, and the corresponding monthly means of (d) F10.7 and (e) 3-hourly Kp indices for the period February 2002 – August 2019. The blue points are yearly averages calculated from different months.

2.2 Data Processing

2.2.1 Removing Seasonal Variation

Multiday period signals are well eliminated by using monthly means. In order to study the long-term trend and solar response of the mesopause temperature, an important question is how to eliminate the seasonal variation from the monthly mean temperature series. Figure1 and Figure2 clearly reveal the presence of a pronounced annual variation at middle and high latitudes with low temperatures during summer and high temperatures during winter. Bittner et al. (2000) applied the maximum entropy method to find dominant frequency components to model the seasonal behavior of the temperatures in the upper mesosphere and reported that annual, semiannual and terannual cycles need to be taken into account when modeling the whole time series. The seasonal variation in temperature is commonly characterized by a sum of an annual, semiannual and terannual harmonics (Bittner et al., 2000; Offermann et al., 2003, 2004, 2010; Perminov et al., 2014; Ammosova et al., 2014; Kalicinsky et al., 2016). Following the method used before in those studies, we perform a three-component harmonic fit analysis on monthly mean temperatures for each latitude bands separately. Then, residual temperatures after removing seasonal variation can be obtained by subtracting the harmonic fit:

$$y_{res}(t) = y(t) - \sum_{i=1}^{3} A_i \sin(\frac{2\pi}{\tau_i} t + \varphi_i) \quad (2)$$

with $\tau_i = 12\text{month}/i$, where $y(t)$ is the measured monthly mean mesopause temperature series, t is the time points in months from the February 2002, A_i and φ_i are the amplitudes and phases of the sinusoids. The calculated residual temperatures with seasonal variation removed for each latitude zone we will use further in the study to analyze the long-term trend and solar response.

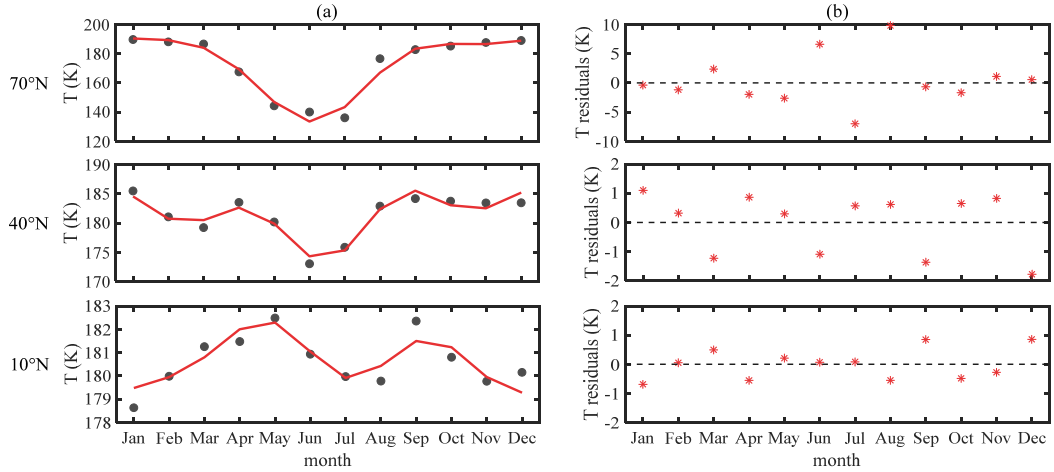

Figure 3. (a) Seasonal variation of a composite year for the 70°N, 40°N, and 10°N. Black solid dots are monthly mean mesopause temperature by averaging all January, February, etc. values from 2002 to 2019. The red solid lines are harmonic fit with annual, semiannual and terannual terms. (b) Temperature residuals obtained by subtracting the seasonal variation from the monthly mean temperatures.

The seasonal variation of a composite year for the 70°N, 40°N, and 10°N latitudes is shown in Figure 3(a) as a typical example, which is indicated by the black solid dots. The composite year of the mesopause temperature is formed by averaging all January, February, etc. monthly means during 2002-2019. Figure 3(a) reveals a clear annual variation at middle to high latitudes and a pronounced semiannual variation at low latitudes with low temperatures during summer and winter and high temperatures during spring and autumn. The red solid lines in Figure 3(a) show their corresponding three-component harmonic fits. Subtraction of the harmonic fit yields the residual temperatures with seasonal cycle removed plotted in Figure 3(b).

2.2.2 Detecting Long-term Trends and Solar Responses

The long-term trend and solar response can be determined for each latitude bin by using multiple linear regression (MLR) model to the seasonal variation removed temperature residuals with terms of constant, time, F10.7, Kp. This model takes the following terms:

$$y_{\text{res}}(t) = a + b \cdot t + c \cdot s(t) + d \cdot s(t)^2 + f \cdot k(t) \quad (3)$$

where $y_{res}(t)$ is the monthly residual mesopause temperature series with seasonal variation removed from the equation (2); t is the monthly time series points since February 2002; $s(t)$ is monthly means of the solar 10.7 cm flux derived from the

equation (1); $k(t)$ is monthly means of the three-hourly Kp index. The constant a, long-term trend b in K/month, F10.7 and Kp term coefficients c, d and f are obtained through least-squares fit for any given latitude bin. A clear saturation effect between the upper atmospheric temperature and F10.7 index at high values of F10.7 has been well explored, which is addressed by adding a quadratic term in the F10.7 dependence in the equation (3). And a similar treatment for F10.7 has been widely used (e.g., Holt & Zhang, 2008; Ogawa et al., 2014).

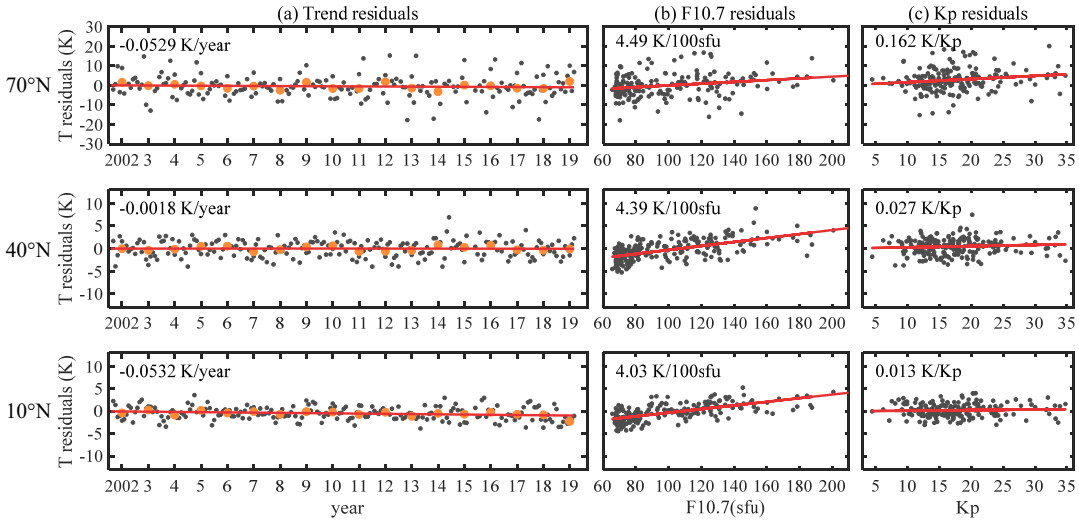

Figure 4. The new secondary T residuals (black dots) generated by removing the other two parameters effects from the seasonally corrected temperature data for (a) long-term trend, (b) F10.7 and (c) Kp in the different latitude bins (top) 70°N, (middle) 40°N and (bottom) 10°N. See the text for more details. Red lines are the least square fit to the black dots. The corresponding fitting slope coefficients are given in the top left corner of each plot. Orange solid dots in Figure 4a are yearly means calculated from different months in every year from 2002 to 2019.

With the equation (3) and the time series of the residual temperatures after subtracting the seasonal components from the equation (2), new secondary monthly temperature residuals (black dots) and a linear fit (red lines) to them are shown in Figure 4. The secondary trend T residuals (black dots) in Figure 4a are calculated by removing regression values with all terms except for the trend one (i.e., with the constant, solar activity F10.7 and geomagnetic activity Kp terms being subtracted from the seasonally corrected temperatures) for different latitude bins. The yearly means averaging every months of the year from 2002 to 2019 are indicated by orange solid dots. The long-term trend can be easily obtained by using the least-squares linear fitting (red line) to these T residual points with time. The results in K/year are presented in the top left corner of each plot. As suggested by previous studies (e.g., Hood et al., 1991), the chemical composition and thermal structure of the middle atmosphere could be affected by the periodic changes during the solar cycle. Thus, the solar cycle influence on temperature should be filtered properly when one detects the long-term temperature trend (Beig, 2002). In this study, the obtained temperature long-term trend has filtered out the solar influence by subtracting F10.7 related terms from the residual temperatures. Clear cooling trends can be seen in Figure 4a and they change with latitude.

The temperature residuals related to F10.7 (black dots) in Figure 4b are generated by subtracting all regression terms except for the F10.7 terms in the equation (3). A least-square fit to them is shown by the red line and the solar response in K/100sfu is

given in the top left corner of each plot. The positive relation between the mesopause temperature and the solar cycle is a signature feature. Similarly, the Kp temperature residuals (black dots) in Figure 4c are calculated by subtracting all regression terms except for the Kp one. A linear fit to them is shown in red line with its fitting slope coefficients in K/Kp shown in the top left corner of the plot by the black text.

In this way, the obtained long-term trend of the mesopause temperatures has been eliminated the seasonal, solar and geomagnetic effects. Similarly, the solar response also has been removed the seasonal, long-term trend and geomagnetic components. We will discuss the latitudinal variation of the long-term trend and solar response in the following sections and provide some brief discussion on the results.

3. Results and Discussion

3.1 SABER Measured Mesopause Temperatures

The Monthly averaged mesopause temperatures derived from SABER measurements for different latitude bins from February 2002 to August 2019 are shown in Figure 1. The mesopause temperature is the coldest point of the monthly averaged SABER temperature profiles between 80 km and 110 km. The monthly variability of mesopause temperatures is similar from year to year. Note that, at high latitudes, there is a clear colder summer level in both hemispheres as indicated in Figure 1. For example, in the northern hemisphere, the mesopause temperature at high latitudes (60°N—80°N) drops in summer months from May to August with mean of 151 K and picks up in the other non-summer months with a mean of 183 K, which is consistent with the two-level structure of mesopause locations. This structure is in general agreement with lidar observations of the mesopause presented by She and von Zahn (1998) as well as in suit falling spheres and Na lidar measurements performed by Lübken and von Zahn (1991). They explained the extremely low temperatures at the pole mesopause in summer are caused by adiabatic upward motion connected with a global scale meridional circulation which is set up by the interaction of breaking gravity waves with the zonal mean flow (Lübken & von Zahn, 1991). Based on Figure 1, we group the mesopause temperatures data into two sets according to month. The mesopause during the summer months (May, June, July, and August for the northern hemisphere; November, December, January, and February for the southern hemisphere) is categorized as “cold mesopause”, mostly dominated by the adiabatic cooling, and the other during the non-summer months as “warm mesopause”, mainly controlled by the radiative cooling process (Yuan et al., 2019). In the following subsections, we will describe the long-term trend and solar response variability with respect to these two kinds of mesopause temperatures.

3.2 Mesopause Temperature Long-term Trends

3.2.1 Latitudinal Variations

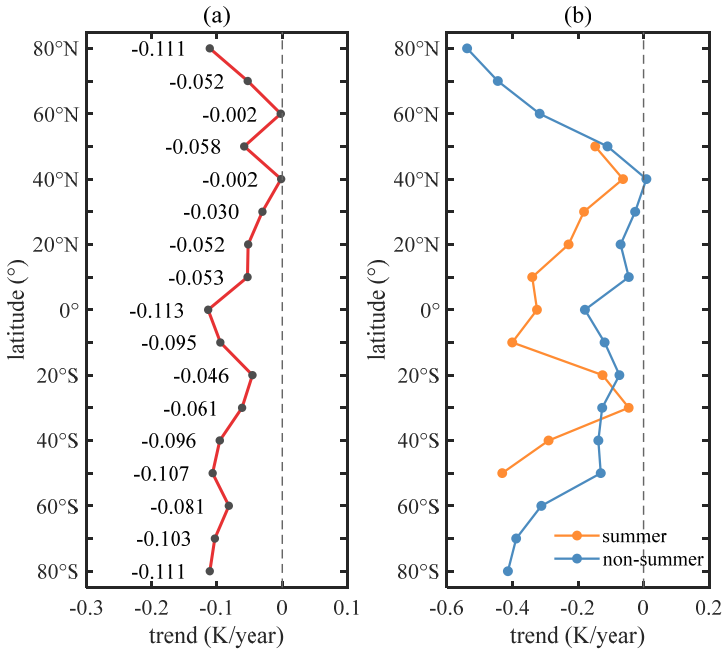

Figure 5. (a) The mesopause temperature trends as a function of the latitude for the time interval of 2002 – 2019. The trends for each latitude are given in black text on the left side of the curve. (b) Latitudinal variation of the mesopause temperature trends for summertime and non-summer time. The orange line indicates the summertime trends in K/year and the blue line the non-summer trends. The straight dashed line shows the zero line.

In Figure 5, we present results for the long-term trend variability with latitude after removing seasonal, solar cycle and geomagnetic activity influences as described in the previous section. The mesopause temperature trends shown in Figure 5a are derived from all available monthly data spanning over 18 years from February 2002 to August 2019 at each latitude. The results in K/year are presented on the left side of the curve with black text. Very clear cooling trends can be seen throughout the entire latitude range except for 40°N and 60°N where the values are only slightly below 0 K/year. The trends change with latitude and are stronger (toward negative) at the equator and high latitudes. The cooling trend in the southern hemisphere is observed to be stronger as compared to that in the northern hemisphere. The pronounced cooling trend in the southern hemisphere may be related with a strengthening eastward flow in the southern high latitude polar vortex as a result of ozone photochemical depletion, which reduces the penetration of upward planetary waves into southern winter mesosphere (French & Burns, 2004; Andrew et al., 2012). The derived cooling trend is in the range of -0.002 to -0.113 K/year with a mean of -0.069 ± 0.036 K/year in Figure 5a, implying the global mesopause temperature reduction over the past eighteen years from 2002 to the present time is in the range of 0.036 – 2.03 K. This is consistent with the conclusion suggested by Laštovička et al. (2006) that the upper atmosphere is generally cooling and contracting. And they also indicated that the dominant driver of these cooling trends in the upper atmosphere is increasing greenhouse forcing. In the mesopause region (80 – 100 km), doubling of CO_2 leads to 5 – 6 K cooling on a globally averaged basis (Beig et al., 2003). Additionally, based on model calculation, Bremer and Berger (2002) pointed out that mesospheric temperature trends are influenced not only by the increase of greenhouse gases (CO_2) but also by a decrease of the atmospheric ozone (O_3). Additionally, the known

potential drivers to some extent also include anthropogenic changes of water vapor and natural long-term variation of geomagnetic activity (Laštovička et al., 2008).

The temperature cooling trend in the mesopause region has been indicated by several past studies (e.g., She et al., 2015; Yuan et al., 2019). However, the temperature cooling trends near the mesopause observed by SABER after subtracting seasonal, solar and geomagnetic components are generally smaller than the temperature trends at heights of 50 to 80 km. The lack of strong cooling trend near the mesopause is consistent with model simulation (Garcia et al., 2007) and agrees reasonably with a variety of observation results (rocketsonde, lidar, satellite, etc.) in the comprehensive review summarized by Beig et al. (2003, 2006, 2011b). It thus appears that the temperature trends near the mesopause are not statistically significant with the order of a few K per year. But they almost agree in sign. As pointed out by Beig (2011b), various trend analysis results reported by different workers are a snapshot of the time period covered. The period of measurements is not identical in these results, hence, which could lead to different trends in magnitude obtained by different investigators.

The mesopause temperature exhibits a distinct summer/non-summer difference at high latitudes in both hemispheres. As mentioned in section 3.1, we here define the summertime as May-August for the northern hemisphere and November-February for the southern hemisphere corresponding to the "cold mesopause"; the non-summer time as the rest months corresponding to the "warm mesopause". Figure 5b shows the trend derived from a least-square linear fitting using summertime and non-summer time temperature residuals respectively. In general, the non-summer trend first decreases gradually from the equator to low and middle latitudes for both hemispheres and then show a sharply increasing cooling with latitude extending to poleward. These cooling trends at high latitudes are statistically significant. At 80°N and 80°S latitude, the non-summer cooling trend reaches the local maximum with the trend of -0.53 K/year and -0.41 K/year, respectively. The temperature trends for summer months show apparent cooling trend at low and middle latitudes of 50°N – 50°S and are stronger than those for non-summer months at almost latitudes except for 30°S. Summer trends for the latitudes from 60° to 80° in both hemispheres are not presented here, as the results are statistically insignificant. With falling sphere measurements (69°N) and rocket grenade (~70°N) data for the altitude range 50 – 85 km, Lübken (2000, 2001) also reported negligible temperature trends during summer for high latitudes. Similarly, using the ground-based hydroxyl (OH) temperatures observed at Stockholm (59.5°N, 18.2°E) from 1991 to 1998, Espy and Stegman (2002) examined the trends on a month to month basis and revealed no significant trend during the high-latitude polar summer.

3.2.2 Monthly Variations

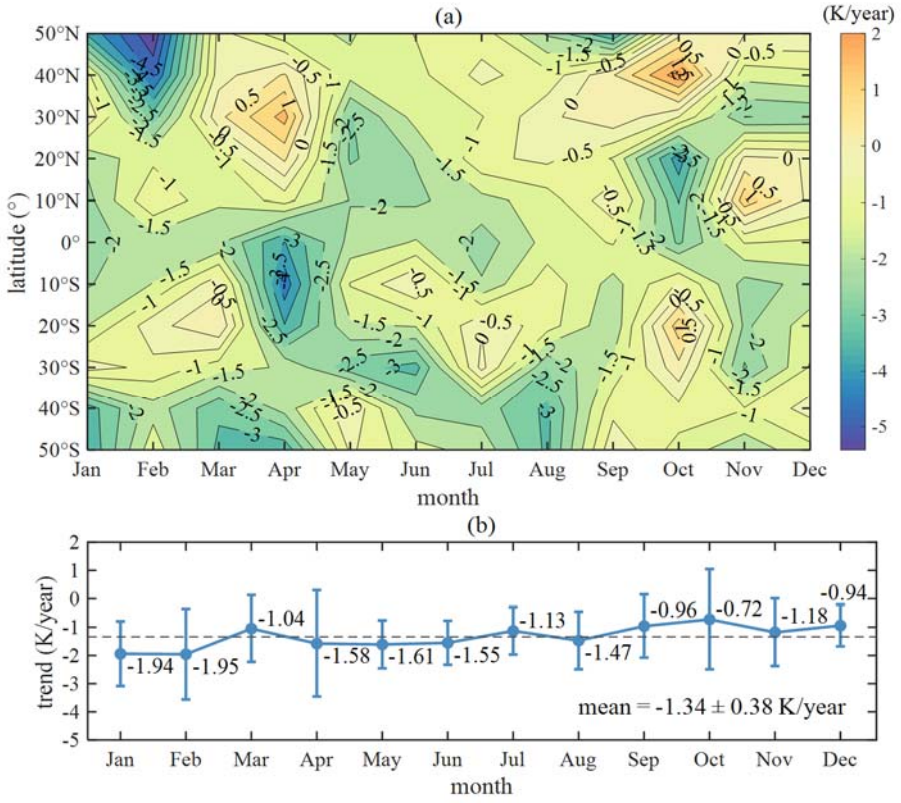

Figure 6. (a) Latitude versus month variations of the mesopause temperature long-term trend. Contours are marked with trend values at a 0.5 K/year unit interval between -4 K/year and 2 K/year. (b) The corresponding means of long-term temperature trends (K/year) for each month during the course of the year. The vertical bars indicate the fluctuation range of trends at different latitudes from 50°N to 50°S. The annual mean of the monthly trend points is shown by the dashed line and the mean value is shown by black text in the lower right corner of the plot.

Monthly trends can be obtained by sorting data with different years in the time interval 2002 – 2019 according to the month. Figure 6a gives a monthly variation of the mesopause temperature long-term trends at different latitudes ranging from 50°N to 50°S with every 10° interval and their means from every latitude bins of each month are plotted in Figure6b. For poor data completeness caused by the instrument yaw cycle and failure, the monthly results obtained at high latitudes 60° – 80° in both hemispheres are not included here. The trends are more variable from one month to another, especially in the northern hemisphere than in the southern hemisphere. At 50°N latitude, for example, the trend exhibits a characteristic semiannual variation with stronger cooling in February and September, and slightly weaker cooling or even warming in other months. This variation is similar to the monthly long-term temperature trends result (Figure 9) published by Offermann et al. (2010) who used upper mesosphere (87 km) hydroxyl (OH) temperatures at Wuppertal (51°N, 7°E) in 1987-2008. Note that, however, the amplitude of monthly trends centered at 50°N in Figure 6 is larger than Offermann's (Offermann et al., 2010, their Figure 9). In addition to different data sources, different data coverage could also lead to this difference, which will be discussed in the following section. At 30°N – 50°N latitude, there is a remarkable cooling trend observed in February and a prominent warming trend in October. They are symmetrical about June. It is interesting to note that there are another two similar distributions that are symmetrical about summertime. One pair is the apparent warming that emerges in April centered at 30°N with a corresponding cooling in October at 20°N. The other pair is located in the southern hemisphere with

a prominent cooling in April at 10°S and moderate warming in October at 20°S. The result shown in Figure 6a indicates that the behavior of mesopause temperature long-term trends is generally hemispherically symmetric at low and middle latitudes. The monthly trend curve presented in Figure 6b shows large trend differences between a moderate cooling of -0.72 K/year in October to a deep cooling of -1.95 K/year in February. The annual mean of the shown points is -1.34 ± 0.38 K/year. They are all below 0 K/year, exhibiting cooling trends during the course of the year. The trend fluctuations shown by the vertical bars are larger during the spring and autumnal equinox periods as compared with those during summer and winter seasons, which could be caused by strong dynamic forcing in the mesopause region during equinox months over the global. The gravity waves and the planetary waves propagate upward and equatorward more effectively at equinox, breaking and depositing their energy in the uppermost mesosphere (Remsberg et al., 2008), and contribute to enhanced vertical mixing.

3.2.3 Solar Activity Dependency

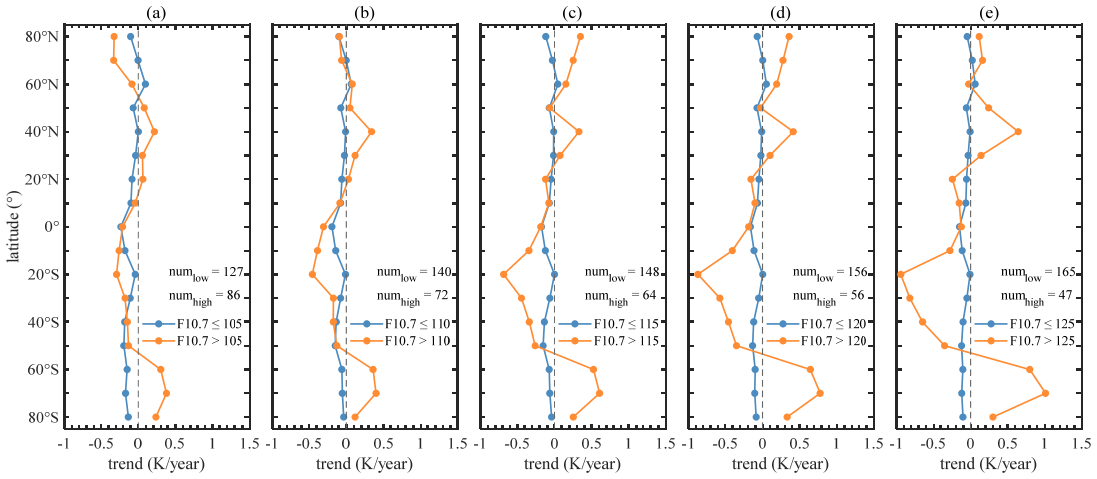

Figure 7. Latitudinal distribution of the long-term temperature trends for low solar activity and high solar activity divided by F10.7 at (a) 105, (b) 110, (c)115, (d)120, (e)125 respectively. Black text is the number of the corresponding data points.

Figure 7 provides the latitudinal variation of temperature trends derived from the trend residuals with F10.7 indices divided into two levels at 105, 110, 115, 120, 125 respectively. The corresponding number of data points are shown by the black text in each plot. These numbers include a little missing data at each latitude as indicated in Figure 1. Compared with high solar activity indicated by the orange line in Figure 7, the variation of the trends as a function of F10.7 shows little variability for low solar activity. And a relatively stable cooling exists throughout the almost entire latitude ranging from 80°N to 80°S for low solar activity where the trends are below or slightly above (only 60°N) 0 K/year. However, the variation of the trends for high solar activity shows varied and large variability with latitude. And these variations are observed being stronger with F10.7 increasing. At 60°N – 80°N latitude, the trends shift to warming from cooling trend when F10.7 indices are larger than 115 sfu. And the apparent increasing warming occurs at 30°N – 50°N latitude with the highest warming 0.64 K/year appearing at 40°N for F10.7 beyond 125 sfu. Interestingly, for the variation of the trends as a function of F10.7, a reverse transition from slightly warming to cooling appears at 20°N latitude. And strong increasing cooling exists throughout the latitude range from 10°N to 50°S with the deepest cooling -0.94

K/year at 20°S latitude for F10.7 reaching beyond 125. The trends, however, between 60°S – 80°S behave differently again with apparent warming. And this warming trend increases rapidly with increasing F10.7 especially at 70°S latitude reaching 1.01 K/year. The different behavior of trends at different latitudes between low F10.7 index and high F10.7 index indicates that the enhanced solar activity can cause the trend to be strengthened no matter cooling or warming, implying the trend dependence on solar activity is more significant at high solar activity than low solar activity.

3.3 Mesopause Temperature Solar Responses

3.3.1 Latitudinal Variations

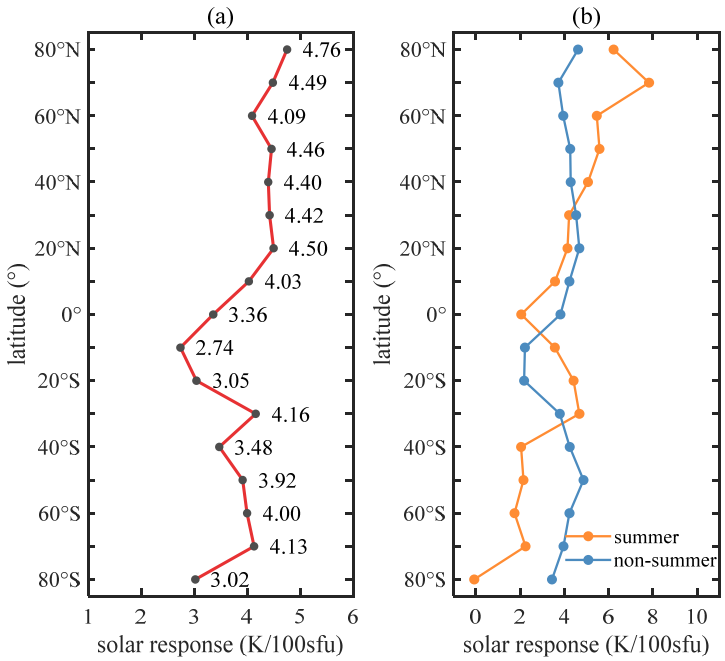

Figure 8. (a) Solar responses at different latitudes ranging from 80°N to 80°S with every 10° interval. The solar response for each latitude is provided by black text on the right side of the curve. (b) Solar responses at different latitudes for summertime and non-summer time. The orange line indicates the summertime solar responses in K/100sfu and the blue line of the non-summer solar responses.

According to the method mentioned in Section 2.2, we obtain the solar responses at each latitude from 80°N to 80°S, which are derived from temperature residuals as shown in Figure 4b with the seasonal cycle, constant term, long-term trend and geomagnetic activity removed. The results are shown in Figure 8a and solar responses for each latitude in K/100sfu are given by the black text on the right side of the curve. And Figure 8b shows the corresponding summer and non-summer solar response for each latitude. Months of May-August in the northern hemisphere and November-February in the southern hemisphere are considered for summer. As shown in Figure 8a, the curve shows positive solar responses throughout the entire latitudes with a maximum of 4.76 K/100sfu at 80°N and a minimum of 2.74 K/100sfu at 10°S, implying a positive correlation between temperature and solar activity. The mean value of the shown solar response points is 3.94 ± 0.59 K/100sfu. The lower responses of the temperature to solar radio flux F10.7 with the order of 2 – 3 K/100sfu generally are observed at equatorial to middle latitudes in the southern hemisphere, while the larger values are found throughout the northern hemisphere with ~4 K/100sfu. Figure 8a indicates stronger mesopause solar responses in the northern

hemisphere than the southern hemisphere. This latitudinal distribution is consistent with the previous mesopause region (80 – 100 km) solar response results summarized in the review by Beig (2011a). The expected significant positive results obtained here are consistent with other solar response studies. Beig and Fadnavis (2009) has reported the temperature analysis of rocketsonde from Thumba (8°N, 77°E), India during the period 1971 – 1993 and found solar response being negative in the stratosphere and positive in the mesosphere with a distinct boundary around 52 – 54 km. A significant positive solar response of 3.5 ± 0.2 K/100sfu over Wuppertal (51°N, 7°E) is reported by Offermann et al. (2010) who used OH airglow measurements during the period 1987 – 2008 to derive the temperature near the mesopause region. Similarly, positive solar responses are also found in lidar datasets over Fort Collins (41°N, 105°W) during 1990 – 2007 in the mesopause region (She et al., 2009) and in the satellite-based temperature measurements as well as model results between ± 83° (Forbes et al., 2014). However, the magnitude of solar response in recent literature is reported to be different, which may be caused by the different seasonal distribution of observation as solar response at the mesopause is highly seasonally dependent (Offermann et al., 2004; Golitsyn et al., 2006). In addition, the differences in temperature response to solar activity are mainly caused by changes in the vertical distribution of chemically active gases and by changes in UV irradiation as well as the intervention of dynamics (Beig et al., 2008).

The mesopause temperature response to solar activity is more variable in the southern hemisphere than in the northern hemisphere. This behavior, to some degree, can be explained by Figure 8b which shows that the difference of the solar response between summer and non-summer time is greater in the southern hemisphere as compared to that in the northern hemisphere, leading to a variable variation in the overall solar responses in the southern hemisphere as shown in Figure8a. In general, solar responses in the northern hemisphere are more significant in magnitude than those in the southern hemisphere. And the mesopause temperature responses on solar activity near the equator region are relatively weaker than the mid-high latitudes as shown in Figure 8a. In the review of the mesospheric and lower thermospheric temperature response to solar activity, Beig et al. (2002, 2008, 2011a) also reported that temperature solar response in the mesopause region appears to be relatively weaker for the tropical region. The lower solar activity sensitivity in this region may be associated with the relatively weaker correlation between the mesopause temperature and the F10.7 index near the equator shown in Figure 9c. This suggests that besides solar activity influence, there appears strong dynamical forcing from tides at low latitudes (at tropics), where tidal amplitudes are large (Beig et al., 2003; Remsberg et al., 2008).

3.3.2 Monthly Variations

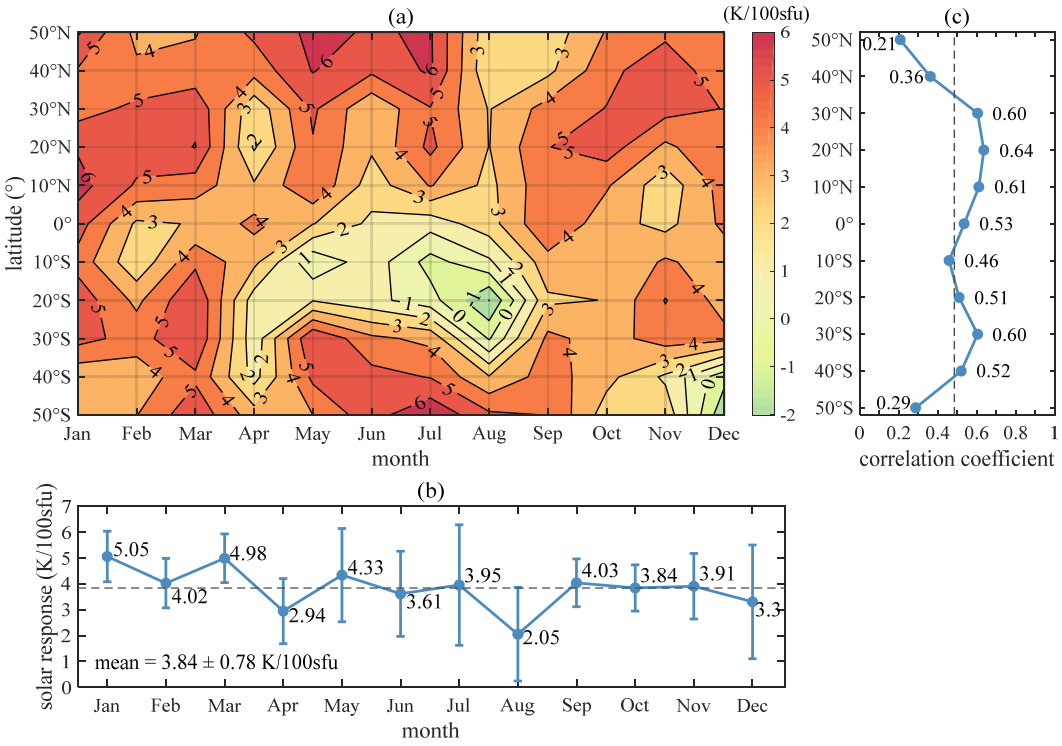

Figure 9. (a) Monthly variation of mesopause temperature solar responses at different latitudes ranging from 50°N to 50°S. The contour interval is 1 K/100sfu. (b) The corresponding means of solar responses for each month during the course of the year. The vertical bars indicate the fluctuation range of solar responses at different latitudes from 50°N to 50°S. The annual mean of the monthly solar response points is shown by the dashed line and the mean value is shown by black text in the lower-left corner of the plot. (c) Latitudinal distribution of correlation coefficients between the monthly mesopause temperature and the monthly F10.7 index. The black text shows the correlation coefficients at better than 99% significance at different latitudes. Gray dashed line indicates the mean correlation coefficient.

Figure 9a further provides the monthly variations of solar responses at different latitudes ranging from 50°N to 50°S during the course of the year. The monthly solar response is calculated by sorting monthly data series, temperature residuals and the corresponding F10.7 indices, from different years during the period of 2002 – 2019 according to the calendar month. Results for high latitudes (60° – 80°) are not included here for poor statistical robustness due to small numbers of sampling points in several months. From Figure 9a, we can see that solar responses have apparently different behavior between the two hemispheres. In general, significant and stable positive temperature responses are observed during all seasons throughout the northern hemisphere. And they vary slightly from month to month with a smaller swing of 0.33 K/100sfu at a mean level of 4.46 K/100sfu. In the southern hemisphere, however, solar response changes considerably with season (even in sign). The negative temperature response to solar activity is observed during August in 20°S – 30°S latitude bins and during December in 40°S – 50°S latitude bins. The mean solar response throughout the southern hemisphere is relatively small: 3.32 K/100sfu with a larger fluctuation of 0.81 K/100sfu as compared to those in the northern hemisphere. The sign of the solar response changes depending not only on latitude but also on the season.

We then calculate solar response means of every month from different latitudes and the results are shown in Figure 9b. The monthly sensitivity of mesopause temperature to solar radio flux shows apparent variation during the course of the year varying from

the smallest 2.05 K/100sfu in August to the largest 5.05 K/100sfu in January. The annual mean solar response as indicated by the gray dashed line is 3.84 ± 0.78 K/100sfu, suggesting a mesopause temperature swing of 4.3 ± 1.19 K from solar radio flux minimum to maximum in a cycle of 153 sfu (65 to 218 sfu). Offermann et al. (2004) also reported different solar influences during different months of the year from OH temperatures measured at Wuppertal (51°N, 7°E) and the mean sensitivity is 3.0 ± 1.6 K/100sfu, which is similar with our result. The observed seasonal distinction of the mesopause temperature to solar activity is conceivably linked with the vertical distribution of some chemically active gas components and the changes of the solar UV radiation (Golitsyn et al., 2006).

By using correlation analysis, we further obtain the correlation coefficients of the monthly series between raw mesopause temperature and the corresponding F10.7 index for every latitude bin ranging from 50°N to 50°S with every 10° interval, as shown in Figure 9c. The latitudinal distribution of the correlation coefficient is symmetrical about 10°S. The correlation coefficients gradually increase first from the equator to the mid-low latitudes and then sharply decrease from the middle latitudes to the poles in both hemispheres, presenting an M shape. This M feature is consistent with the finding of Tang et. al (2016) who calculated global correlation coefficients between the annual mean mesopause temperature and F10.7 and stated that the correlation coefficients at middle latitude are higher than those of the equator and high-latitude regions. Thus, the monthly mesopause temperature is significantly correlated to F10.7 at low and middle latitudes, implying that when solar activity has an increasing or decreasing tendency, the mesopause temperature over that latitudes regions is generally increasing or decreasing too.

4. Some Further Discussion

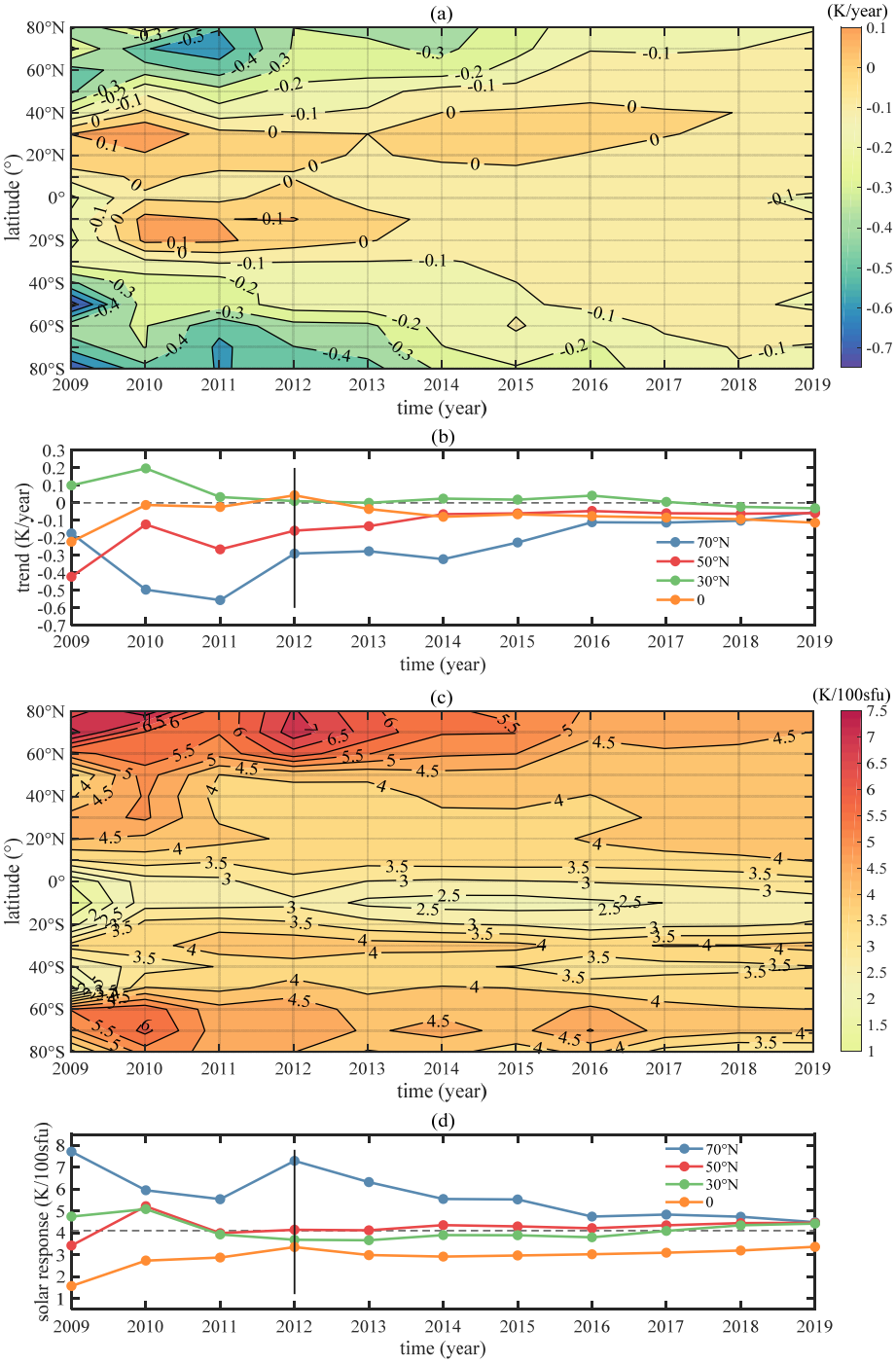

Figure 10. (a) The long-term trends of the mesopause temperature at different latitudes ranging from 80°N to 80°S with every 10° interval in time windows of lengths increasing from 8 to 18 years. Abscissa gives the ending year of the window and runs from 2009 to 2019. The contour interval is 0.1 K/year. (b) Horizontal cut through the upper panel at 70°N, 50°N, 30°N and 0° indicated by the blue, red, green and orange curve respectively. Black vertical line located in 2012 marks the 11-year time interval. Gray dashed line indicates the zero line. (c) As (a) but for solar responses. The contour interval is 0.5 K/100sfu. (d) As (b) but for solar responses. Gray dashed line indicates the mean solar response from the four curves.

In our analysis method of the mesopause temperature long-term trend and solar response, the seasonal effect in the raw monthly temperature data has been removed by subtracting a three-component harmonic fit, yielding the corresponding monthly residual temperatures. The temperature long-term trend derived from the multiple linear regression as given in the equation (3) has subtracted the influence of solar activity and geomagnetic activity. Similarly, the temperature solar response obtained in our results has detrended the influence from the long-term trend and geomagnetic activity. Also, the length of the time interval can be a noteworthy problem when estimating the true long-term trend and solar response in such an analysis. To demonstrate this, we artificially change the length of the time series, using a shorten data window from eight years to eighteen years. The variation of long-term trends and solar response at different latitude bins on an increased length of the data window is shown in Figure 10. The values of the first column are for the window 2002 – 2009 (8 years). The next column values are for the window 2002 – 2010 (9 years). Each forward column includes one more year, and the last one is for the entire data series 2002 – 2019 (18 years). The abscissa indicates the ending year of each data window. Figure 10a shows that an increasing data window gradually improves the stability of the results. The change of the long-term trend is no longer significant with the increasing of the length of the data window throughout all the latitude bins and exhibits a clear symmetrical distribution between the two hemispheres. However, the length of the data window for appearing fairly stable long-term trend differs slightly at different latitudes. To further clearly demonstrate this, horizontal cuts through Figure 10a at 70°N, 50°N, 30°N, and 0° are plotted in Figure 10b, representing the high, middle, low latitude and the equator, respectively. Except for 70°N, a remarkable decrease in the fluctuation of the long-term trends can be observed since 2012 with an 11-year time interval, as indicated by the black vertical line in Figure 10b. This decrease for 70°N is not observed until 2016 with a longer time interval of fifteen years. Then, they all are gradually close to below 0 K/year, presenting slight cooling trends, with the increasing of the length of the time interval. A similar feature is also observed in the variation of the solar response with the increasing length of the time interval at different latitudes as shown in Figure 10c. The mesopause temperature responses to solar activity at high latitudes are more sensitive and significant to the length of the time interval and take a longer time interval to decrease to a stable level as compared with those at middle and low latitudes. As presented in Figure 10d, the stabilization of the variation of the solar response at 70°N latitude only occurs after 2016 when the time interval is longer than fifteen years, while the other three curves can start in the earlier four years since 2012 with an 11-year window marked by the black vertical line. Different lengths of the analysis time interval can lead to different results of the derived long-term trend and solar response. Based on the features at different latitudes presented in Figure 10, we could conclude that a relatively stable long-term trends and solar responses can be obtained with an analysis window only longer than one solar cycle (eleven years) for low and middle latitudes (50°N – 50°S),

and it takes more two to four years with a time interval of 13 – 15 years for high latitudes (60° – 80°). Thus, the analysis window in such analysis needs to be at least longer than one solar cycle, which is also discussed by Offermann et. al (2010) and Kalicinsky et al. (2016).

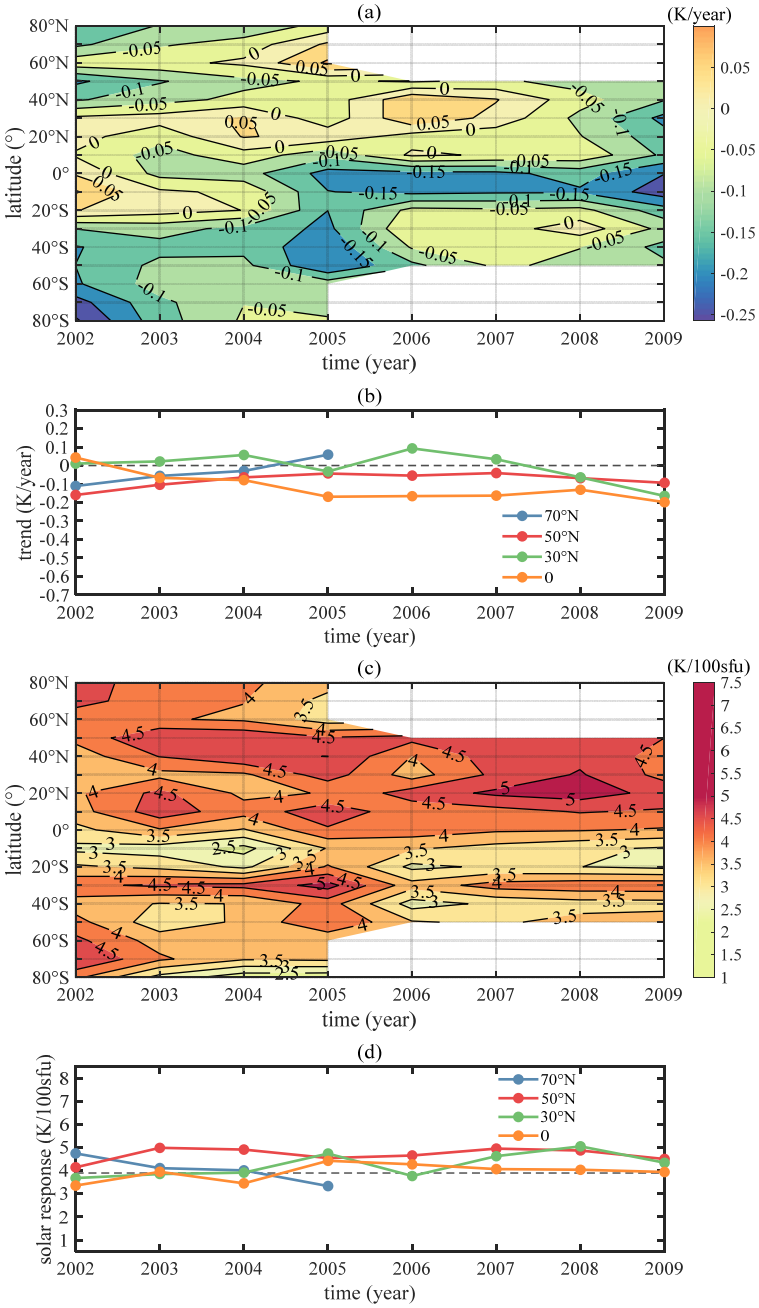

Figure 11. (a) The temperature long-term trends at different latitudes with 11-year time windows for 50°N – 50°S and 15-year for 60° – 80°. Abscissa gives the beginning year of the window shifted through the data interval 2002 – 2019 in steps of one year. The contour interval is 0.05 K/year. (b) Horizontal cut through the upper panel at 70°N, 50°N, 30°N and 0° indicated by the blue, red, green and orange curve respectively. Gray dashed line indicates the zero line. (c) As (a) but for solar responses. The contour interval is 0.5 K/100sfu. (d) As (b) but for solar responses. Gray dashed line indicates the mean solar response from the four curves.

Also, there is another noteworthy matter that whether or not the beginning and ending time of the analysis window, the phases of the solar cycle, influences the derived long-term trend or solar response, after using a long enough time window. To demonstrate this question, based on the results in Figure 10, we first chose a fixed analysis time window of eleven years for 50°N – 50°S and fifteen years for 60° – 80° latitude to calculate the long-term trend and solar response. Then, the time window is moved forward in steps of one year during the past 18 years. We start with the window of 2002 – 2012 for 50°N – 50°S and 2002 – 2016 for 60° – 80° and end with the window of 2009 – 2019 for 50°N – 50°S and 2005 – 2019 for 60° – 80° in both hemispheres. The results are shown in Figure 11. The results derived from a long enough fixed time window show some variation, but the variation is non-significant with the change of the beginning and end of the window. The standard deviation of long-term trends in Figure 11a is 0.075 K/year which is much smaller than the fluctuation of the long-term trends in Figure 10a with a standard deviation of 0.159 K/year. As for the solar response, the standard deviation of the results in Figure 11c is 0.69 K/100sfu which is also much decreased as compared to solar response fluctuation in Figure 10c with a value of 1.05 K/100sfu. The apparent stable variation of the long-term trend and solar response can also be observed in Figure 11b and Figure 11d as compared to the variation of the curves in Figure 10b and Figure 10d, respectively. It suggests that compared with the length of the time window, the variation amplitude of the long-term trends and solar responses caused by changing the beginning or ending time of the window is not significant, and this influence can be ignored though there are still some small variations. Thus, in such analysis, using a long enough time window, an increasing number of sampling points, will guarantee a robust result of the long-term trend or solar response.

The length of the time interval in our analysis is eighteen years that is longer than one solar cycle, to some extent, leading to relatively reliable long-term trends and the solar response of the mesopause temperature for different latitudes. However, the available data sets covering two more solar cycles over the global scale are desired in the future study.

5. Conclusions

The SABER temperature observations between 2002 and 2019 provide eighteen years of continuous temperature data in the mesosphere and lower thermosphere. Using this data, we presented the monthly mean mesopause temperature variations from February 2002 to August 2019 between 83°N and 83°S latitude with every 10° interval. The SABER results demonstrated a two-level structure for the mesopause temperature at high latitudes with a colder temperature during summer, corresponding to the summer lower mesopause height. To investigate the long-term trend and solar response of the mesopause temperature, a three-component harmonic fit (a sum of an annual, semiannual and terannual cycles) was applied first to remove the seasonal variation from the monthly time series temperature data. And then a multiple linear

665 regression and the least-squares method were performed to detect the temperature
666 long-term trends and solar responses.

667 The long-term trends of the mesopause temperatures, after removal of seasonal, solar
668 activity and geomagnetic activity influences, show a cooling trend through all
669 latitudes ranging from -0.002 to -0.113 K/year with a mean of -0.069 ± 0.036 K/year.
670 The general cooling upper atmosphere is believed to be mainly caused by increasing
671 greenhouse gases and the decreasing atmospheric ozone. The trends at the equator and
672 high latitudes are relatively stronger (toward negative) than those at middle and low
673 latitudes. And the cooling trend in the southern hemisphere is observed to be more
674 apparent as compared to that in the northern hemisphere. This stronger cooling trend
675 in the southern hemisphere is reported to be related to the reduction of penetration of
676 upward planetary waves into the southern winter mesosphere as a result of ozone
677 photochemical depletion in the southern polar (French & Burns, 2004; Andrew et al.,
678 2012). Based on SABER observations, stronger negative trends are detected at high
679 latitudes (60°– 80°) in both hemispheres during the non-summer time, and magnitude
680 can be up to -0.53 K per year, while no significant trends are found for summertime at
681 high latitudes. The lack of significant trends during the high-latitude polar summer is
682 consistent with other ground-based observations (Lübken 2000, 2002; Espy &
683 Stegman, 2002). The monthly temperature trends for the latitude of 0°– 50° in two
684 hemispheres show large variability during the course of the year and even appear a
685 slight warming trend in some months. An analysis of the sensitivity of the long-term
686 trend to solar activity suggests that there is no significant influence of solar activity on
687 temperature trends during low solar activity, while high solar activity will strengthen
688 the corresponding temperature trend.

689 The temperature solar responses near the mesopause, with the seasonal cycle, long-
690 term trend and geomagnetic activity influences removed, show an apparent positive
691 response to solar activity through all latitudes ranging from 2.74 (10°S) to 4.76
692 K/100sfu (80°N) with mean of 3.94 ± 0.59 K/100sfu. The positive solar response also
693 implies a positive correlation between temperature and solar activity. The solar
694 response in the northern hemisphere is observed to be more significant and stable in
695 contrast to the relatively weak and variable southern solar response discussion. There
696 is an apparent drop in solar response near the equatorial region, which could be
697 caused by strong dynamical forcing from tides at low latitudes, where tidal amplitudes
698 are relatively large (Beig et al., 2003; Remsberg et al., 2008). The monthly solar
699 response shows considerable variation during the course of the year at different
700 latitudes, and their means vary from the minimum 2.05 K/100sfu in August to the
701 maximum 5.05 K/100sfu in January. The distinct variation from month to month is
702 linked with the vertical distribution of some chemically active gas components and
703 the changes of the solar UV radiation at different seasons (Golitsyn et al., 2006).

704 It is noteworthy that, in such an analysis of temperature long-term trend and solar
705 response, the length of the time window and the phase of the solar cycle should be

treated with caution, as they will lead to different results even for the same data source. A robust and stable result of long-term trend or solar response could be obtained only when the length of the analysis time window is longer than 11 years (one solar cycle) for low and middle latitudes (50°N – 50°S) and 13 – 15 years for high latitudes (60° – 80°). The phase of the solar cycle also has an influence on long-term trends or solar responses, but it is not as remarkable as the effect of the time interval used. Thus, we conclude that the length of the time interval chosen for analysis is the main factor guaranteeing the quality of the results. In this study, our results are for an eighteen years interval of 2002 – 2019, which are expected to be a reference to the temperature variation near the mesopause. However, the available data sets covering multiple solar cycles are desired in the future to reveal and verify the possible physical mechanism and any underlying process of the temperature trend in the upper mesosphere.

Acknowledgments

The study was partly supported by the National Natural Science Foundation of China (Grant no. 41875045) and supported by Hunan Provincial Innovation Foundation for Postgraduate (CX2018B034).

We are grateful to the SABER scientific team for permission to use the SABER data. The version 2.0 level 2A data set of SABER is downloaded from ftp://saber.gats-inc.com/Version2_0/Level2A/. The solar radio flux index F10.7 and geomagnetic activity index Kp are download from http://celestrak.com/SpaceData/.

References

Ammosov, P., Gavrilyeva, G., Ammosova, A., & Koltovskoi, I. (2014). ScienceDirect Response of the mesopause temperatures to solar activity over Yakutia in 1999 – 2013. *Advances in Space Research*, *54*(12), 2518–2524. https://doi.org/10.1016/j.asr.2014.06.007

Andrew, Thomas, J. B., Hosking, J. S., Thomas, J., Joanna, D. H., Tony, P., & Wuhu, F. (2012). Possible dynamical mechanisms for southern hemisphere climate change due to the ozone hole, 69, 2917–2932. https://doi.org/10.1175/JAS-D-11-0210.1

Beig, G. (2002). Overview of the mesospheric temperature trend and factors of uncertainty. *Physics & Chemistry of the Earth*, *27*, 509–519.

Beig, G. (2006). Trends in the mesopause region temperature and our present understanding — an update. *Physics & Chemistry of the Earth*, *31*, 3–9. https://doi.org/10.1029/2002RG000121

Beig, G. (2011a). Long - term trends in the temperature of the mesosphere / lower thermosphere region : 2 . Solar response. *Journal of Geophysical Research*, *116*, A00H12. https://doi.org/10.1029/2011JA016766

Beig, G. (2011b). Long - term trends in the temperature of the mesosphere / lower thermosphere region :1.Anthropogenic influences. *Journal of Geophysical Research Atmospheres*, *116*, A00H11. https://doi.org/10.1029/2011JA016646

Beig, G., & Fadnavis, S. (2009). Solar response in the temperature over the equatorial middle atmosphere. *Journal of Atmospheric and Solar-Terrestrial Physics*, *71*, 1450–1455. https://doi.org/10.1016/j.jastp.2008.07.07

Beig, G., Keckhut, P., Lowe, R. P., Roble, R. G., Mlynczak, M. G., Scheer, J., … Bremer, J. (2003). Review of mesospheric temperature trends. *Reviews of Geophysics*, *41*(4), 1015. https://doi.org/10.1029/2002RG000121

Beig, G., Scheer, J., Mlynczak, M. G., & Keckhut, P. (2008). Overview of the temperature response in the mesosphere and lower thermosphere. *Reviews of Geophysics*, *46*, RG3002. https://doi.org/10.1029/2007RG000236.

Berger, U., & Lübken, F. J. (2011). Mesospheric temperature trends at mid - latitudes in summer, *38*, L22804. https://doi.org/10.1029/2011GL049528

Berger, U., & Zahn, U. Von. (1999). The two-level structure of the mesopause: A model study. *Journal of Geophysical Research*, *104*(D18), 22083–22093.

Bittner, M., Offermann, D., & Graef, H. H. (2000). Mesopause temperature variability above a midlatitude station in Europe. *Journal of Geophysical Research Atmospheres*, *105*(D2), 2045–2058.

Brasseur, G. p., & Solomon, S. (2005). *Aeronomy of the Middle Atmosphere: Chemistry and Physics of the Stratosphere and Mesosphere*. Springer.

Bremer, J., & Berger, U. (2002). Mesospheric temperature trends derived from ground-based LF phase-height observations at mid-latitudes : comparison with model simulations. *Journal of Atmospheric and Solar-Terrestrial Physics*, *64*, 805–816.

Espy, P. J., & Stegman, J. (2002). Trends and variability of mesospheric temperature at high-latitudes. *Physics & Chemistry of the Earth*, *27*, 543–553.

Forbes, J. M., Zhang, X., Marsh, D. R. (2014). Solar cycle dependence of middle atmosphere temperatures. *Journal of Geophysical Research Atmospheres*, *119*, 9615–9625. https://doi.org/10.1002/2014JD021484.Received

French, W. J. R., & Burns, G. B. (2004). The in uence of large-scale oscillations on long-term trend assessment in hydroxyl temperatures over Davis , Antarctica. *Journal of Atmospheric and Solar-Terrestrial Physics*, *66*, 493–506. https://doi.org/10.1016/j.jastp.2004.01.027

Garcia, R. R., Marsh, D. R., Kinnison, D. E., Boville, B. A., & Sassi, F. (2007). Simulation of secular trends in the middle atmosphere , 1950 – 2003. *Journal of Geophysical Research*, *112*, D09301. https://doi.org/10.1029/2006JD007485

Golitsyn, G. S., Semenov, A. I., Shefov, N. N., & Khomich, V. Y. (2006). The response of middle-latitudinal atmospheric temperature on the solar activity during various seasons. *Physics and Chemistry of the Earth*, *31*, 10–15. https://doi.org/10.1016/j.pce.2005.03.001

Holt, J. M., & Zhang, S. R. (2008). Long-term temperature trends in the ionosphere above Millstone Hill. *Geophysical Research Letters*, *35*, L05813. https://doi.org/10.1029/2007GL031148

Hood, L. L., Huang, Z., & Bougher, S. W. (1991). Mesospheric effects of solar ultraviolet variations: further analysis of SME IR ozone nimbus 7 SAMS temperature data. *Journal of Geophysical Research*, *96*(D7), 12989–13002.

Kalicinsky, C., Knieling, P., Koppmann, R., Offermann, D., Steinbrecht, W., & Wintel, J. (2016). Long-term dynamics of OH^* temperatures over central Europe : trends and solar correlations. *Atmospheric Chemistry and Physics*, *16*, 15033–15047. https://doi.org/10.5194/acp-16-15033-2016

Laštovička, J., Akmaev, R. A., Beig, G., Bremer, J., & Emmert, J. T. (2006). Global Change in the Upper Atmosphere. *Science*, *314*, 1253–1254. https://doi.org/10.1016/j.jastp.2006.03.008

Laštovička, J., Akmaev, R. A., Beig, G., Bremer, J., Emmert, J. T., Jacobi, C., Jarvis, M.J., Nedoluha, G., Portnyagin, Yu. I., & Ulich, T. (2008). Annales Geophysicae Emerging pattern of global change in the upper atmosphere and ionosphere. *Annales Geophysicae*, *26*, 1255–1268.

Lübken, F., Berger, U., & Baumgarten, G. (2013). Temperature trends in the midlatitude summer mesosphere. *Journal of Geophysical Research Atmospheres*, *118*, 13347–13360. https://doi.org/10.1002/2013JD020576

Lübken, F. J. (2000). Nearly zero temperature mesosphere trend in the polar summer mesosphere. *Geophysical Research Letters*, *27*(21), 3603–3606.

Lübken, F. J. (2001). No long term change of the thermal structure in the mesosphere at high latitudes. *Advances in Space Research*, *28*(7), 947–953.

Lübken, F. J., & von Zahn, U. (1991). Thermal Structure of the Mesopause Region at Polar Latitudes. *Journal of Geophysical Research*, *96*, 20841–20857.

Mertens, C. J., Russell, J. M., Mlynczak, M. G., She, C., Schmidlin, F. J., Goldberg, R. A., Lopez-Puertas, M., Wintersteiner, P. P., Picard, R. H., Winick, J. R. & Xu, X. (2009). Kinetic temperature and carbon dioxide from broadband infrared limb emission measurements taken from the TIMED / SABER instrument. *Advances in Space Research*, *43*, 15–27. https://doi.org/10.1016/j.asr.2008.04.017

Offermann, D., Donner, M., Knieling, P., Hamilton，K., Menzel, A., Naujokat, B., & Winkler, P. (2003). Indications of long-term changes in middle atmosphere transports. *Advances in Space Research*, *32*(9), 1675–1684.

Offermann, D., Donner, M., Knieling, P., & Naujokat, B. (2004). Middle atmosphere temperature changes and the duration of summer. *Journal of Atmospheric and Solar-Terrestrial Physics*, *66*, 437–450. https://doi.org/10.1016/j.jastp.2004.01.028

Offermann, D., Hoffmann, P., Knieling, P., Koppmann, R., & Oberheide, J. (2010). Long - term trends and solar cycle variations of mesospheric temperature and dynamics. *Journal of Geophysical Research Atmospheres*, *115*, D18127. https://doi.org/10.1029/2009JD013363

Ogawa, Y., Motoba, T., Buchert, S. C., Häggström, I., & Nozawa, S. (2014). Upper atmosphere cooling over the past 33 years. *Geophysical Research Letters*, *42*, 5629–5635. https://doi.org/10.1002/2014GL060591.

Perminov, V. I., Semenov, A. I., Medvedeva, I. V., & Pertsev, N. N. (2014). Emission Observations at Midlatitudes Temperature Variations in the Mesopause Region According to the Hydroxyl Emission Observations at Midlatitudes. *Geomagnetism and Aeronomy*, *54*(2), 230–239. https://doi.org/10.1134/S0016793214020157

Remsberg, E. E., Marshall, B. T., Garcia-Comas, M., Krueger, D., Lingenfelser, G. S., Mlynczak, M. G., Russell, J. M., Smith, A. K., Zhao, Y., Brown, C., Gordley, L. L. L., Lopez-Gonzalez, M. J., Lopez-Puertas, M., She, C. Y., Taylor, M. J., & Thompson, R. E. (2008). Assessment of the quality of the Version 1 . 07 temperature- versus-pressure profiles of the middle atmosphere from TIMED / SABER. *Journal of Geophysical Research Atmospheres*, *113*, D17101. https://doi.org/10.1029/2008JD010013

Richards, P. G., Fennelly, J. A., & Torr, D. G. (1994). EUVAC: A solar EUV flux model for aeronomic calculations. *Journal of Geophysical Research Atmospheres*, *99*(A5), 8981–8992.

Roble, R. G., & Dickinson, R. E. (1989). How will changes in carbon dioxide and methane modify the mean structure of the mesopause and thermosphere? *Geophysical Research Letters*, *16*(12), 1441–1444.

Russell, J. M. I., Mlynczak, M. G., Gordley, L. L., Tansock, J., & Esplin., R. (1999). An Overview of the SABER Experiment and Preliminary Calibration Results. *Proceedings of SPIE*, *3756*, 277–288. https://doi.org/10.1117/12.366382.

Semenov, A. I. (2002). The season peculiarities of behaviour of the long-term temperature trends in the middle atmosphere on the mid-latitudes. *Physics & Chemistry of the Earth*, *27*, 529–534.

She, C., Krueger, D. A., Akmaev, R., Schmidt, H., Talaat, E., & Yee, S. (2009). Atmospheric and Solar-Terrestrial Physics Long-term variability in mesopause region temperatures over Fort Collins , Colorado (41.1°N , 105.1°W) based on lidar observations from 1990 through 2007, *71*, 1558–1564. https://doi.org/10.1016/j.jastp.2009.05.007

She, C., Krueger, D. A., & Yuan, T. (2015). Long-term midlatitude mesopause region temperature trend deduced from quarter century (1990 – 2014) Na lidar observations. *Annales Geophysicae*, *33*, 363–369. https://doi.org/10.5194/angeocom-33-363-2015

She, C. Y., & Zahn, U. Von. (1998). Concept of a two-level mesopause : Support through new lidar observations. *Journal of Geophysical Research*, *103*, 5855–5863.

Smith, A. K. (2004). Physics and chemistry of the mesopause region. *Journal of Atmospheric and Solar-Terrestrial Physics*, *66*, 839–857. https://doi.org/10.1016/j.jastp.2004.01.032

Tang, C., Liu, D., Wei, H., Wang, Y., Dai, C., Wu, P., Zhu, W., & Rao, R. (2016). The response of the temperature of cold-point mesopause to solar activity based

on SABER data set. *Journal of Geophysical Research: Space Physics*, *121*, 7245–7255. https://doi.org/10.1002/2016JA022538.Received

Venkat Ratnam, M., Patra, A. K., & Krishna Murthy, B. V. (2010). Tropical mesopause : Is it always close to 100 km ? *Journal of Geophysical Research Atmospheres*, *115*, D06106. https://doi.org/10.1029/2009JD012531

Xu, J., Smith, A. K., Yuan, W., Liu, H. L., Wu, Q., Mlynczak, M. G., & Russell, J.M. (2007). Mesopause structure from Thermosphere , Ionosphere , Mesosphere , Energetics , and Dynamics (TIMED)/ Sounding of the Atmosphere Using Broadband Emission Radiometry (SABER) observations. *Journal of Geophysical Research Atmospheres*, *112*, D09102. https://doi.org/10.1029/2006JD007711

Yuan, T. (2019). The Long - Term Trends of Nocturnal Mesopause Temperature and Altitude Revealed by Na Lidar Observations Between 1990 and 2018 at Midlatitude Journal of Geophysical Research : Atmospheres. *Journal of Geophysical Research Atmospheres*, *124*, 5970–5980. https://doi.org/10.1029/2018JD029828